INVESTIGATION OF THERMAL STRESS CONVECTION IN NONISOTHERMAL GASES UNDER MICROGRAVITY CONDITIONS

Daniel W. Mackowski and Roy W. Knight
Mechanical Engineering Department, Auburn University, AL 36849

ABSTRACT

Microgravity conditions offer an environment in which convection in a nonisothermal gas could be driven primarily by thermal stress. A direct examination of thermal stress flows would be invaluable in assessing the accuracy of the Burnett terms in the fluid stress tensor. We present a preliminary numerical investigation of the competing effects of thermal stress, thermal creep at the side walls, and buoyancy on gas convection in nonuniformly heated containers under normal and reduced gravity levels. Conditions in which thermal stress convection becomes dominant are identified, and issues regarding the experimental measurement of the flows are discussed.

INTRODUCTION

Kinetic theory of gases predicts that temperature gradients can be constitutively related to fluid stresses. These effects, referred to as thermal stress, are described by the Burnett contributions to the fluid stress tensor, which in turn constitutes the second–order approximation in Knudsen number Kn ($= l/L$, where l is the gas mean–free path and L is the characteristic system length) to the Boltzmann equation – the Navier–Stokes equations representing the first–order approximation.[1] To date, the main application of the Burnett terms in fluid mechanics modeling has been to extend the range of validity of continuum–based formulations to transitional Knudsen regimes ($0 < Kn < O(1)$) and highly nonequilibrium conditions (i.e., large temperature gradients). For example, inclusion of the Burnett terms have been shown to improve the accuracy of calculated velocity and temperature fields for hypersonic flow as compared to conventional Navier–Stokes formulations.[2] Even in such situations, however, the contributions of the Burnett terms to fluid stress are relatively small compared to those arising from velocity gradients. Likewise, the effect of thermal stress in non–isothermal, slow–moving gases under normal gravity conditions will typically be negligible compared to buoyant forces.

One situation where thermal stress can become a primary convection mechanism in a nonisothermal gas is the microgravity environment. Beginning with Rosner in 1989, several investigations have been performed to determine the effects of thermal stress (and the often–more–important mechanism of thermal creep at the container side walls) on vapor transport in μg crystal growth processes.[3–5] However, a direct observation of convection that results from thermal stress, which would be possible in a buoyancy–free environment, would be of key interest in itself – in that it would provide highly useful information towards assessing the validity of the Burnett terms.

The objective of our work is to assess the feasibility of such an approach. Specifically, we intend to conduct detailed numerical investigations of gas convection in closed, nonuniformly heated containers, with the goal of identifying optimum conditions for the generation and measurement of thermal stress flows. This paper presents some preliminary results from our investigation.

MODEL AND FORMULATION

As a starting point, we consider the simple system in which a gas is contained within a cylindrical enclosure with controlled temperature and/or heat flux conditions on all surfaces. The system is taken to be axisymmetric (corresponding to axial–directed gravity and symmetric

boundary conditions) and in steady state. The governing continuity, momentum, and energy equations are

$$\frac{1}{r}\frac{\partial \rho r v}{\partial r} + \frac{\partial \rho u}{\partial z} = 0 \tag{1}$$

$$\frac{1}{r}\frac{\partial \rho r v^2}{\partial r} + \frac{\partial \rho u v}{\partial z} = -\frac{\partial P}{\partial r} + \frac{1}{r}\frac{\partial r \tau_{rr}}{\partial r} + \frac{\partial \tau_{rz}}{\partial z} - \frac{\tau_{\phi\phi}}{r} \tag{2}$$

$$\frac{1}{r}\frac{\partial \rho r u v}{\partial r} + \frac{\partial \rho u^2}{\partial z} = -\frac{\partial P}{\partial z} + \frac{1}{r}\frac{\partial r \tau_{rz}}{\partial r} + \frac{\partial \tau_{zz}}{\partial z} - \rho g \tag{3}$$

$$\frac{1}{r}\frac{\partial \rho c_p r v T}{\partial r} + \frac{\partial \rho c_p u T}{\partial z} = \frac{1}{r}\frac{\partial}{\partial r} r k \frac{\partial T}{\partial r} + \frac{\partial}{\partial z} k \frac{\partial T}{\partial z} \tag{4}$$

in which u and v are the axial and radial components of velocity.

The effect of thermal stress will appear in the fluid stress tensor $\boldsymbol{\tau}$, which will be comprised of the 'classical' Newton–Stokes relations and the higher–order Burnett terms. Since the flows will be relatively slow–moving, the only significant Burnett terms will be those corresponding to temperature gradients. With this approximation, the thermal stress contribution to the stress tensor appears[5,6]

$$\boldsymbol{\tau}_T = -\frac{\mu^2 \mathcal{R}}{P}\left[\omega_3\left(\nabla\nabla T - \frac{1}{3}(\nabla^2 T)\,\mathbf{I}\right) + \frac{\omega_5}{2T}\left((\nabla T)(\nabla T) - \frac{1}{3}(\nabla T \cdot \nabla T)\,\mathbf{I}\right)\right] \tag{5}$$

In the above, μ is the dynamic viscosity, $\mathcal{R}$ is the specific gas constant, and ω_3 and ω_5 are Burnett coefficients, which depend on the force interactions between the gas molecules. We assume here the case of Maxwellian molecules, for which $\omega_3 = \omega_5 = 3$.[2]

The velocity boundary conditions on the side and end walls are

$$u(r = R, z) = \frac{C_s \nu}{T}\frac{\partial T}{\partial z}\bigg)_{r=R}, \quad v(r = R, z) = 0 \tag{6}$$

$$u(r, z = 0, L) = 0, \quad v(r, z = 0, L) = \frac{C_s \nu}{T}\frac{\partial T}{\partial r}\bigg)_{z=0,L} \tag{7}$$

in which C_s is a dimensionless coefficient that has the value of 3/4 for Maxwellian molecules with complete accommodation. The velocity slip conditions in the above are typically referred to as 'thermal creep'. In the results presented herein, we neglect the effects of temperature jump and viscous slip at the wall – which will be appropriate for near–continuum (i.e., $Kn \ll 1$) conditions.

The gas is taken to be monatomic (with $Pr = 2/3$), and we assume that the dynamic viscosity varies with temperature according to $\mu \propto T^{0.72}$.[2] In all presented results we have used Burnett and creep coefficients for Maxwellian molecules.

Numerical solution of Eqs. (1–4) was accomplished using the SIMPLE algorithm.[7] A non–uniform mesh, typically of 21 and 41 nodes in the radial and axial directions, respectively, was employed. Discretization of the thermal stress source terms in the momentum equations followed the control volume procedure as outlined in Ref. 7. Inclusion of the third–order temperature derivatives in the thermal stress terms would, in principle, require the specification of additional thermal boundary conditions at the surfaces. However, energy transport is dominated by conduction for the slow–moving conditions of the system. The energy equation thus becomes effectively decoupled from the momentum equations, which results in a second–order system for the temperature field.

In all cases, the presented results for temperature and velocity are within 0.5% of the values obtained when the grid spacing was halved. Results from the code for free convection heat transfer in cylindrical enclosures were found to be in acceptable agreement with previously published values. We are unaware of previously published numerical calculations for thermal stress convection for similar conditions to those examined here.

Calculation Results

Calculations were performed on a system corresponding to helium at 1 atm pressure in a $L = 2$ cm, $R = 1$ cm container. The end walls at $z = 0$ and $z = L$ were isothermal at 300 and 600 K, respecitvely. The side wall was maintained at 300 K, except for a 1 mm adiabatic strip adjacent to the hot end of the container. The rationale for the thermal conditions is to devise a system which minimizes temperature gradients along the surfaces (which drive creep flows along the surfaces) while maintaining relatively large temperature gradients in the bulk gas (the source of thermal stress). In this regard, an 'ideal' situation would have the top and side walls of the container at uniform yet different temperatures.[6] Such a condition, however, is both physically unrealistic and numerically troublesome – and we therefore include the 1 mm adiabatic length between the cold and hot surfaces.

Figure 1 shows calculated isotherms and dimensionless velocity vectors for a system at unit gravity (directed towards the cold end). The origin of the container in the velocity vector plot is in the lower left corner, and the legend refers to the scale of the velocity arrow in units of ν_C/L, where ν_C is the kinematic viscosity of the gas at the cold temperature (≈ 2 cm^2/s for helium at STP). Thermal creep is seen to result in a strong recirculation of the gas along the adiabatic section of the side wall, whereas buoyancy leads to a counter–rotating vortex within the main section of the container. Reduction of g to 10^{-3} results in the apparent disappearance of the buoyant recirculation, as seen in Fig. 2. However, magnification of the velocity scale by a factor of 20 reveals the convection pattern created by thermal stress, which is shown in the right–hand plot. The vectors directly within the thermal creep recirculation zone have been removed here, to avoid 'spilling' into the rest of the plot. The magnitude of the predicted velocities generated from thermal stress for the given conditions, at around $0.1\nu_C/L \approx 1$ mm/s, are consistent with order–of–magnitude estimations by Viviani et al..[5] Results for zero gravity are essentially unchanged from those appearing in Fig. 2.

To distinguish between the flows resulting from thermal creep and thermal stress, we present in Fig. 3 vector plots of the flows calculated with thermal stress and without thermal creep (a, left), and with creep and without stress (b, right). The values of g is the same as in the previous plot. By comparison of Figs. 3b and 2, one sees that thermal stress in the primary source of convection in all but the adiabatic corner of the enclosure. It is difficult to draw any general conclusions regarding the recirculation generated by thermal stress – except that it is considerably more complicated than that generated by buoyancy. In Fig. 3a the largest velocities generated by stress act somewhat similar to those produced by creep at the side wall, in that the flow is pushed along the adiabatic section of the wall towards the hot end of the enclosure. However, a second recirculation pattern results in a flow of gas along the wall towards the cold end. Additional calculations (not shown here) have indicated that the nature of the thermal stress recirculation is strongly dependent on the value of the hot/cold temperature ratio, the length of the adiabatic zone, and the variation of viscosity with temperature.

Flow Measurement Issues

A concurrent task in our work will be to identify feasible means of measuring gas velocities that result from thermal stress convection in μg conditions. Methods based on the tracking of small seed particles in the gas, such as LDV, would generally be biased by thermophoretic motion of the particles – which would be significant in the highly nonisothermal conditions of an experiment. However, since particle sedimentation is not as critical an issue in the μg environment as it is on earth, relatively large particles – with correspondingly lower thermophoretic diffusivities – could be used to track the flow.

To further examine this concept, we calculated the trajectories of 'test' particles that were released into flowfields calculated under various thermal and gravitational conditions. Assuming that the particles have zero inertia and zero Brownian motion, the positions of the particles are obtained by integration of the motion equations:

$$\frac{dr_p}{dt} = v - \frac{f_T \nu}{T}\frac{\partial T}{\partial r} \tag{8}$$

$$\frac{dz_p}{dt} = u - \frac{f_T \nu}{T}\frac{\partial T}{\partial z} - B m_p g \tag{9}$$

where f_T is a thermophoretic diffusion factor for the particle, B is the particle mobility, and m_p is the particle mass. For spherical particles of radius a_p, the mobility and thermophoretic factors are approximated as[8]

$$B = \frac{f_c}{6\pi\mu a_p} \tag{10}$$

$$f_T = \frac{2 f_c C_S(\phi + C_t Kn_p)}{(1 + 3C_m Kn_p)(1 + 2\phi + 2C_t Kn_p)} \tag{11}$$

where $Kn_p = l/a_p$ is the particle Knudsen number, $\phi = k_g/k_p$ is the ratio of gas and particle thermal conductivities, C_m and C_t (≈ 1.14 and 2.2) are the momentum exhange and temperature jump coefficients, and f_c is the Millikan correction factor,

$$f_c = 1 + Kn_p\,(1.2 + 0.41\exp(-0.88/Kn_p)) \tag{12}$$

An increasing correspondence between the particle trajectory and the flow streamlines is obtained by reducing both f_T and $m_p g$. Equation (11) shows that former can be reduced by increasing both particle size and particle thermal conductivity. Using, for example, a 10 μm aluminum particle ($\phi \approx 0.001$, $Kn_p \approx 0.03$ for helium at 450 K, 1 atm) gives a thermophoretic factor $f_T \sim 0.07$ – which results in roughly comparable magnitudes of particle thermophoretic and thermal stress convective velocities for the conditions modelled in the previous section. Calculated trajectories for the particle, which is released at the point $r^*_{p,0} = 0.1$ and $z^*_{p,0} = 1$, are shown in Fig. 4a. The flow conditions correspond to those presented in Fig. 2, except with unit, 10^{-2}, 10^{-3}, and zero gravity levels. Shown in Fig. 4b are results calculated under identical conditions, except with the absence of thermal stress convection in the flow field.

In unit gravity, the trajectory of the particle is controlled mainly by gravitational forces, and to a lesser extent buoyant recirculation of the gas. However, at lower gravity levels both thermophoresis and thermal stress convection are shown to have a significant effect on the particle trajectory. Since the temperature fields calculated with and without thermal stress are essentially

identical, differences in the trajectories shown in Figs. 4a and b therefore result entirely from the action of thermal stress convection.

SUMMARY

Our preliminary calculations indicate that thermal stress convection in gases could be isolated and examined in the microgravity environment. Of course, much remains to be performed to completely assess the feasibility of an experiment towards this end. Our future work will examine various strategies of heating an enclosed gas – with the objective of identifying methods which maximize the predicted convection from thermal stress while minimizing thermal creep at the walls. For example, it may be desirable to heat a gas via localized absorption of radiation – as opposed to maintaining different temperatures on the walls of the container. We will also further explore particle tracking methods for measurement of the gas convective velocities. Finally, the 'inverse' problem needs to be examined, i.e., given measurements of convective flows in nonisothermal, μg conditions, what can be said about the veracity of the Burnett contributions to the fluid stress tensor?

REFERENCES

1. S. Chapman, and T. G. Cowling, *The Mathematical Theory of Non–Uniform Gases*, Cambridge University Press, London, 1970.

2. X. Zhong, R. W. MacCormack, and D. R. Chapman, "Stabilization of the Burnett Equations and Application to Hypersonic Flows,", *AIAA J.*, **31**, 1036–1043, 1993.

3. D. E. Rosner, "Side wall gas 'creep' and 'thermal stress convection in microgravity experiments on film growth by vapor transport," *Phys. Fluids* **A1**, 1761, (1989).

4. L. G. Napolitano, A. Viviani, and R. Savino, "Fluid dynamic modelling of crystal growth from vapour," *Acta Astronautica* **28**, 197, (1992).

5. A. Viviani, and R. Savino, "Recent developments in vapour crystal growth fluid dynamics," *J. Crystal Growth* **133**, 217, (1993).

6. M. N. Kogan, "Molecular Gas Dynamics," in *Annual Review of Fluid Mechanics*, M. Van Dyke and W. G. Vincenti, Eds., Annual Review, Palo Alto, 1973, Vol. 5, pp. 383.

7. S. V. Patankar, *Numerical Heat Transfer and Fluid Flow*, McGraw-Hill, N.Y., 1980.

8. L. Talbot, R. K. Cheng, R. W. Schefer, and D. R. Willis, "Thermophoresis of particles in a heated boundary layer," *J. Fluid Mech.* **101**, 737, (1980).

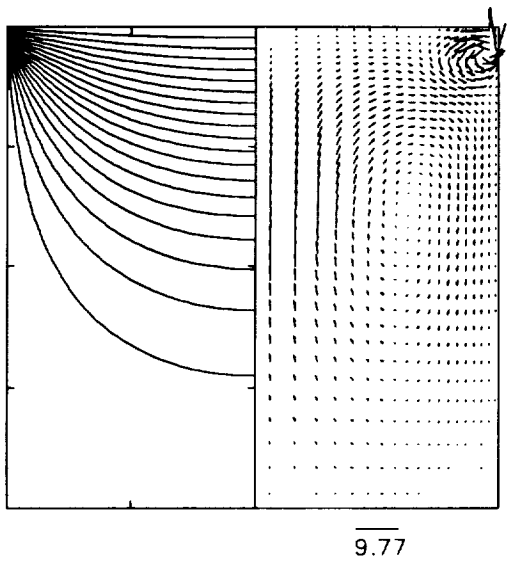

Fig. 1. Isotherms and velocity vectors, unit gravity.

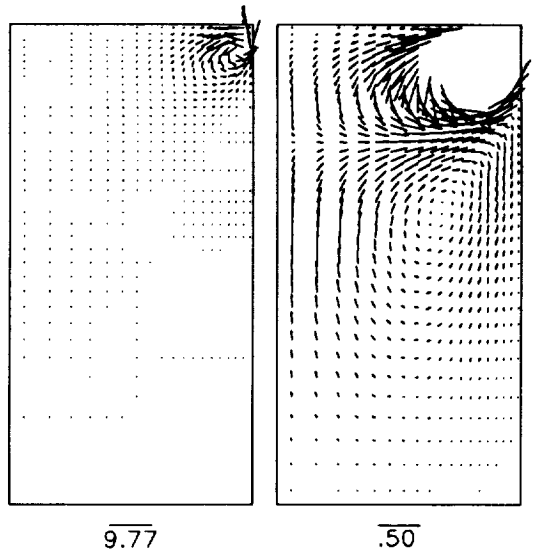

Fig. 2. Velocity vectors, reduced gravity

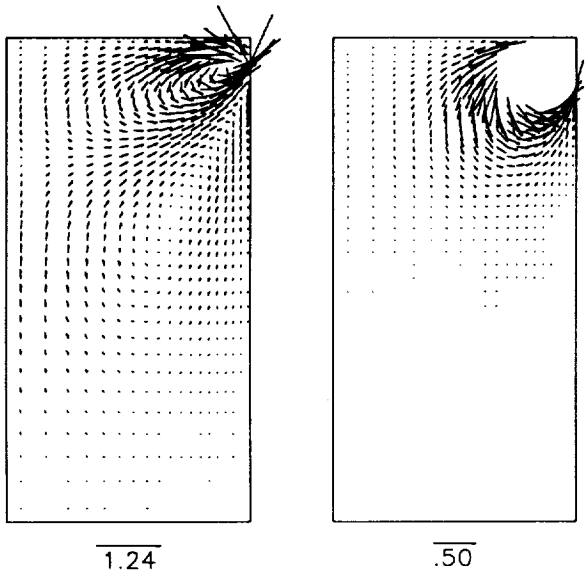

Fig. 3. Separate effects of thermal stress (left) and creep (right)

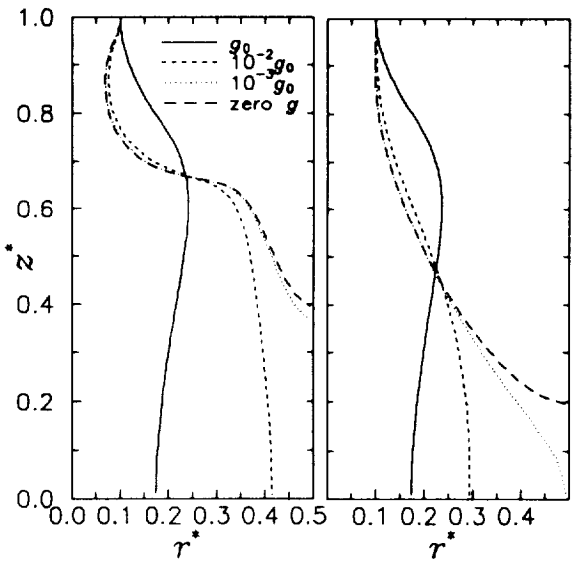

Fig. 4. Particle tracks with (left) and without (right) thermal stress